Environmental Science & Technology

Article

pubs.acs.org/est

Investigating Primary Marine Aerosol Properties: CCN Activity of Sea Salt and Mixed Inorganic−Organic Particles

Stephanie M. King,[†] Andrew C. Butcher,[†] Thomas Rosenoern,[†,▽] Esther Coz,[‡] Kirsten I. Lieke,[†] Gerrit de Leeuw,[§,∥,⊥] E. Douglas Nilsson,[#] and Merete Bilde*[,†]

[†]Department of Chemistry, University of Copenhagen, DK-2100 Copenhagen, Denmark

[‡]Departamento de Medio Ambiente, CIEMAT, E-28040 Madrid, Spain

[§]Climate Change Unit, Finnish Meteorological Institute, FI-00560 Helsinki, Finland

[∥]Department of Physics, University of Helsinki, FI-00560 Helsinki, Finland

[⊥]Department of Air Quality and Climate, TNO Built Environment and Geosciences, NL-3508 TA Utrecht, Netherlands

[#]Department of Applied Environmental Science, Stockholm University, SE-11418 Stockholm, Sweden

Supporting Information

ABSTRACT: Sea spray particles ejected as a result of bubbles bursting from artificial seawater containing salt and organic matter in a stainless steel tank were sampled for size distribution, morphology, and cloud condensation nucleus (CCN) activity. Bubbles were generated either by aeration through a diffuser or by water jet impingement on the seawater surface. Three objectives were addressed in this study. First, CCN activities of NaCl and two types of artificial sea salt containing only inorganic components were measured to establish a baseline for further measurements of mixed organic−inorganic particles. Second, the effect of varying bubble residence time in the bulk seawater solution on particle size and CCN activity was investigated and was found to be insignificant for the organic compounds studied. Finally, CCN activities of particles produced from jet impingement were compared with those produced from diffuser aeration. Analyses indicate a considerable amount of organic enrichment in the jet-produced particles relative to the bulk seawater composition when sodium laurate, an organic surfactant, is present in the seawater. In this case, the production of a thick foam layer during impingement may explain the difference in activation and supports hypotheses that particle production from the two methods of generating bubbles is not equal.

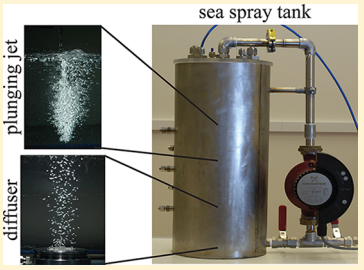

1. INTRODUCTION

The oceans, covering 71% of the Earth's surface, are a large source of atmospheric particles. Particles of marine origin are produced directly from the ocean surface and referred to as primary particles or indirectly via nucleation or condensation of low-volatility gas-phase molecules and referred to as secondary particles. Activity at the ocean surface leading to ejection of primary marine particles includes whitecaps, or sea spray initiated by wind shear, and the subsequent bursting of bubbles formed from the entrainment of air into the ocean water. The global annual mass emission of primary marine particles, or sea spray aerosol (SSA), is estimated to range from 2×10^{12} to 1×10^{14} kg yr^{-1}, which is comparable to that of dust aerosol.[1]

The conventional assumption that SSA consists primarily of sea salt has been challenged in recent years, particularly in the case of submicrometer particles, which may contribute over 90% of the particle number.[2] Studies of in situ samples (e.g., Cavalli et al.[3]) and laboratory sea spray tank experiments (e.g., Keene et al.[4]) have reported not only that submicrometer SSA particles contain organic matter but also that the organic fraction may increase with decreasing size, i.e., from a few percent for particles approximately 1 μm in diameter to >70% for particles having a diameter of roughly 100 nm.[5] The question of organic enrichment has led to efforts to experimentally reproduce the formation of particles from bubble bursting using tanks in which bubble plumes are generated using various methods, including aeration through diffusers and plunging water jets.[4,6−9]

The potentially large fraction of organic matter in marine particles may alter our understanding of the role of marine particles in cloud formation. Marine particles are generally considered efficient cloud condensation nuclei (CCN), i.e., seeds on which water vapor can condense to form cloud droplets, due to their size and hygroscopicity.[10−12] This implies that they have a large influence on cloud droplet number and size in the marine environment and hence on determinations of the aerosol indirect effect of marine particles. Current estimates of the global aerosol indirect effect are associated with large uncertainties,[13] and these may be attributed in part to a lack of sufficient knowledge about the background natural aerosol,

Special Issue: Marine Boundary Layer: Ocean Atmospheric Interactions

Received: February 10, 2012
Revised: July 13, 2012
Accepted: July 18, 2012
Published: July 18, 2012

such as SSA. Recent sea spray tank studies have investigated the CCN activity of particles produced from bubble bursting and have suggested that the effect of organic enrichment on CCN activity is not significant.[14,15] These results are not surprising since theoretical and experimental evidence show that even a small amount of salt has a dominant effect on CCN activity,[16] and an organic fraction greater than 50% in the particle phase may lead to no more than a subtle change in CCN activity.

In this work we address three factors that can affect CCN properties of particles produced from bubble bursting: 1) the composition of the inorganic fraction, 2) the bubble residence time within the water column, and 3) the bubble generation method and the presence of a foam layer on the water surface.

Given the considerable effect of small amounts of salt, a thorough understanding of CCN activity in the marine atmosphere requires a detailed study of the salt component. Although sea salt consists largely of NaCl, and is therefore often assumed to have similar properties, the minor constituents may alter its aerosol properties. Moreover, the measurement of CCN activity of pure NaCl is complicated by the variations in its morphology as a function of size and rate at which it was processed from a droplet to a crystalline particle.[17,18] In this study, we probe the morphologies and CCN activities of NaCl and artificial sea salt from various production methods, including the sea spray tank.

The use of sea spray tanks for aerosol studies has led to a number of publications during the past decade carrying significant climate implications. One concern is the effect of bubble residence time within the water column, which is much shorter in the laboratory setting than those produced by breaking ocean waves.[19] Fuentes et al.,[6] addressing this concern, calculated that the time required to reach equilibrium with respect to adsorption of organic matter on the air−water interface of bubbles is much shorter than typical bubble residence times in sea spray tanks. Here we report experimental results showing the impact of bubble residence time on size and CCN activity of submicrometer particles.

Finally, the effect of different bubble production methods (i.e., jet impingement and diffuser aeration) on particle physicochemical properties is investigated. Given the complexity of simulating sea spray in the laboratory environment, this study has been conducted in an effort to provide not only insight into CCN properties of sea spray aerosol but also knowledge that can be useful in the design of future studies.

2. EXPERIMENTAL SECTION

2.1. Particle Generation. Particles were generated either by atomization or from bubble bursting. A TSI constant output atomizer (model 3076) was used for atomization of aqueous solutions. Bubble bursting was implemented in a stainless steel tank filled with artificial seawater, which comprised 18.2 MΩ-cm water with known concentrations of inorganic and organic solutes. The tank has a height of 44.5 cm and a diameter of 21.8 cm, and it was filled with 10 L of artificial seawater during experiments, thus giving it a headspace of approximately 5 L.

Bubbles were produced either by aeration through a stainless steel, small-pore diffuser placed within the water column of the tank or by a plunging jet. The jet nozzle was mounted such that the flow had a free fall distance of 13.5 cm directed at a 90° angle with respect to the water surface. A large body of literature can be found on the mechanisms and characteristics of plunging liquid jets.(e.g., refs 20−23)

Size spectra of bubbles produced using the two methods were measured using a mini-BMS (bubble measurement system).[24] The size spectrum shown in Figure 1 for bubbles

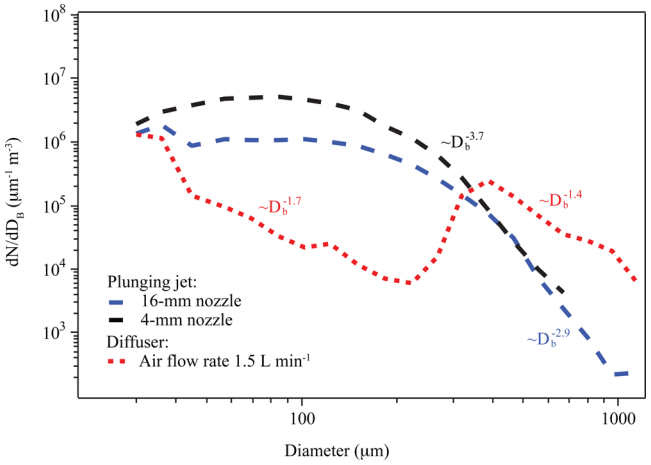

Figure 1. Bubble size distributions produced using the diffuser and the plunging jet in artificial seawater having a salinity (TMSS) of 35‰.

produced using the diffuser at an air flow rate of 1.5 L min^{-1} and at a depth of 26.5 cm below water surface is representative of this type of bubble generation for air flow rates ranging from 0.25 to 2 L min^{-1}. Two nozzle sizes (4 mm and 16 mm) were used to form a plunging jet, with the resulting bubble size spectra shown in Figure 1, along with power law exponents corresponding to the descending portion of each spectrum. Similar to findings from previous sea spray tank studies,[6,8,25] we find that the shape of the jet-generated bubble spectra more closely resemble oceanic bubble size spectra, as determined by power law exponents. Derived roll-off of bubble concentration with respect to radius from the jet closely resemble the acoustic phase of air entrainment in plunging breakers, given in Dean and Stokes[26] as $\propto r^{-1.8}$ to $r^{-2.9}$ per increase in radius below 1 mm. The steeper roll-off with increasing bubble diameter implies that the plunging jet in our laboratory could be replicating a slightly aged, acoustic phase plunging breaker.[26] Upon visual comparison of the bubble size distributions for the plunging jets and diffuser with oceanic bubble size distributions,[26−28] we conclude that the plunging jet better simulates plunging breaking waves with respect to bubble plume characteristics.

2.2. Materials. Artificial seawater solutions were prepared by dissolving either NaCl or artificial sea salt in deionized water. The sea salt proxies included a commercially available Tropic Marin sea salt (TMSS) and a mixture prepared in the laboratory (LSS) from analytical grade salts. Although the exact salt composition of TMSS was not made available, it was confirmed by the manufacturer that no organic compounds are present. The ionic mass ratios of Na^+, Cl^-, Mg^{2+}, HCO^{3-}, and SO_4^{2-} in LSS were comparable to those in natural seawater (i.e., the salt mixture contained, by mass, 73.6% NaCl (Sigma Aldrich, >99.5%), 14.5% $MgCl_2$ (Sigma Aldrich, >98%), 11.5% Na_2SO_4 (Sigma Aldrich, >99%), and 0.4% $NaHCO_3$ (Sigma Aldrich, >99.7%)).[29]

To generate mixed inorganic−organic particles during bubble-bursting experiments, a known amount of an organic compound was added to the artificial seawater in the tank. In a number of the experiments, salinity was reduced well below the

average ocean salinity of 35‰ so that it would not dominate CCN activity, i.e., a reduction in CCN activity was useful for further analysis. The organic compounds used in this study were chosen for their similarity to organic matter typically found in ocean water, such as fatty acids and saccharides,[30,31] or for their surfactant properties. The following compounds were used: palmitic acid (PA, Sigma Aldrich, >99%), sodium laurate (NaLa, Sigma Aldrich, 99-100%), fructose (Fr, Fluka, >99%), mannose (Ma, Fluka, >99.5%), sodium dodecyl sulfate (SDS, Sigma Aldrich, >99%).

Fatty acid salts were included in this study because of their solubility, which is typically higher than that of the corresponding fatty acid. SDS is likely more surface-active than compounds found in the oceans, but it is used here to demonstrate the possible effect of a very strong surfactant.

2.3. Electron Microscopy. Polydisperse particles produced from bubble bursting were sampled from the tank headspace and directed into a silica-gel diffusion dryer. Atomized particles were first mixed with dry, clean air before entering the dryer. A filter holder with a polycarbonate filter (Nucleopore, 0.1 μm pores) was used to collect the dried particles for scanning electron microscopy (SEM). Monodisperse aerosol populations were generated by passing the dried particles through a ^{85}Kr bipolar charger and a differential mobility analyzer (DMA, TSI 3081) before filter collection. The filters were stored under clean and dry conditions to prevent contamination and adsorption of water layers. SEM images were obtained using a Quanta 200 FEG Environmental SEM (Center for Electron Nanoscopy, Technical University of Denmark), which was operated at an acceleration voltage of 5 kV, a spot size of 3 nm, and a working distance of 6 mm.

The collection method for analysis with transmission electron microscopy (TEM) was identical, with the exception that the dried particles were deposited onto Cu-TEM grids with carbon foil (Plano GmbH). Transmission electron microscopy was performed using a FEI CM 20 equipped with an Olympus Veletta CCD camera (Niels Bohr Institute, University of Copenhagen). The instrument was operated at 200 kV under high vacuum conditions.

The images were analyzed for aspect ratio (AR), which is a common parameter reported from two-dimensional image projections of particles, such as those from electron microscopy. It is defined as the ratio of the longest to the shortest dimension of a particle, calculated here by fitting an ellipse to the projected particle area and dividing the major by the minor axis.[32] Therefore, spherical particles have AR of 1, while particles with more cubic or rectangular shapes have AR greater than 1. AR has been used to quantitatively describe particle morphology in field and laboratory studies[33−37] and has been included in a radiative transfer model of dust that incorporates nonsphericity corrections in its parametrization.[38]

2.4. Measurement of CCN Activity and Size Distribution. The flow of particles exiting the silica-gel dryer was split to provide simultaneous size distribution and CCN measurements. All of the instruments following the dryer were contained in a temperature-regulated box, such that the sample temperature did not deviate significantly over the course of the experiments. Size distributions were collected using a scanning mobility particle sizer (SMPS, TSI 3936), where the DMA is preceded by a ^{85}Kr bipolar charger and the sheath-to-aerosol flow ratio of the DMA was 10:1. For CCN measurements, a DMA (TSI 3081, preceded by a ^{85}Kr bipolar charger) was used to select a monodisperse aerosol. The sheath and aerosol flow of the DMA were 10 L min^{-1} and 1.5 L min^{-1}, respectively. The particles exiting the DMA were directed simultaneously to a condensation particle counter (CPC, TSI 3010, 1 L min^{-1}) for measurement of total particle concentration and to the CCN counter (CCNc, Droplet Measurement Technologies, 0.5 L min^{-1}). The experiment was automated using a Labview program designed for CCN measurements, in which a selected range of mobility diameters was scanned by the DMA at selected size and time intervals between each diameter. Scans over a range of CCNc supersaturations were also automated, such that each supersaturation was held constant for a complete scan of mobility diameters.

CCN activation curves are expressed as the ratio of CCN to CPC concentrations measured as a function of dry particle diameter at a fixed supersaturation. Each DMA scan through a complete range of dry diameters yields an activation curve, from which an activation diameter is calculated. Several methods of obtaining the activation diameter have been used in the literature; the method used in this study is based on the model described in Petters et al.[39] This model calculates the transfer function of an ideal DMA and the fraction of multiple-charged particles that pass through the DMA as part of the quasi-monodisperse population that is sampled by the CCNc. An inversion procedure is used to find the activation diameter that yields the best fit of the measured activation data. Figure S1 in the Supporting Information shows some fitted activation curves of atomized ammonium sulfate particles, which were used for calibration of the instrument.

The calibration procedure of the CCNc is similar to those previously described (e.g., Rose et al.[40]), which consists of relating the thermal gradient of the continuous-flow CCNc with the corresponding supersaturation using linear regression. Supersaturation is calculated from the activation diameters of ammonium sulfate using the Aerosol Inorganics Model (AIM)[41,42] to estimate water activity. The thermal gradient is calculated from the reported temperatures in the column and averaged over the measurement period. Averaging of the thermal gradient is also used with experimental measurements, thus any small changes in the temperature control of the CCNc column are accounted for. Moreover, the placement of the CCNc in a temperature-regulated container ensures that the sample temperature does not vary significantly throughout the experiments.

3. RESULTS AND DISCUSSION

3.1. CCN Activity of NaCl and Artificial Sea Salt. The CCN activity of sea salt was measured and compared to that of pure NaCl. Measured critical supersaturations (S_c) and the corresponding activation diameters are shown in Figure 2 for particles produced both by atomization and by bubble bursting. The results show that, regardless of production method (and the accompanying drying method), NaCl particles activated at smaller sizes than sea salt (both TMSS and LSS) particles at the same supersaturation. This observed difference in CCN activity is in agreement with predictions and observations that sea salt particles have lower hygroscopic growth factors than NaCl at RH >75% (i.e., above the deliquescence RH of NaCl).[43,44] Other observed differences include a higher volatility of sea salt relative to NaCl.[43] These observations support the conclusion that the mixture of inorganic compounds in sea salt, though dominated by NaCl, affects the properties of the mixed particle relative to those of NaCl. Results from this study emphasize that, for studies in which CCN analyses are used to infer

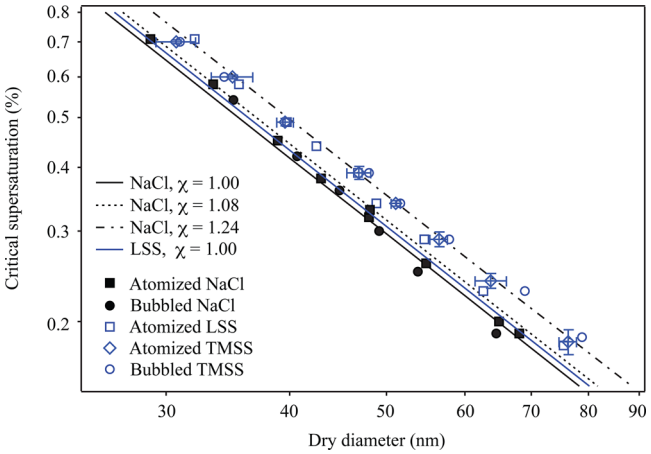

Figure 2. Observed critical supersations of NaCl and artificial sea salt particles. Bubbles were generated using the diffuser in artificial seawater having a salinity of 35‰. Uncertainties for dry diameter and supersaturation are shown for atomized TMSS data and are representative for all the data presented. Uncertainties were calculated as 2 times the standard deviation of measurements of activation diameter and CCNc column temperature gradient, respectively, from repeated experiments. S_c of NaCl particles predicted from Köhler theory for typical χ are also shown, as well as predictions for LSS.

chemical composition and potential organic enrichment, it is important to account for the detailed composition of the sea salt rather than assuming that sea salt can be simply represented by NaCl.

Figure 2 includes theoretical CCN activation curves for NaCl and LSS, calculated from Köhler theory and using the AIM model to estimate water activity. The AIM model used in the case of the multicomponent LSS is based on work by Harvie et al.[45] Under the assumption of dilute conditions at droplet activation, the solution density and surface tension are assumed to be equal to those of water. Dynamic shape factors (χ) are incorporated in the calculations to represent different assumed morphologies of NaCl. Determination of χ, which is the ratio of the drag force on the particle to that on a spherical particle of identical volume,[46,47] is essential in accurate interpretations of data measurements involving the use of a DMA, which classifies particles by electric mobility and whose performance is defined for spherical particles. The nonspherical morphology of NaCl and other salt particles has been discussed in a number of previous studies.[48,49] More recent studies show the effect of particle drying rate and particle size on χ of submicrometer NaCl particles; the range of χ values reported in these studies is wide and indicates that NaCl particle morphologies range from nearly cubic to nearly spherical, depending on size and drying history.[17,18]

The three χ values used to calculate the curves in Figure 2 are 1.00 (i.e., a sphere), 1.08 (i.e., a cube in the continuum regime), and 1.24 (i.e., a cube in the free-molecule regime). Observed CCN activities for NaCl particles from both atomization and bubble bursting are similar to those reported by Wang et al. for fast drying rates (101 RH s^{-1}), i.e., the deviation as a function of size of measured data points for NaCl from the model line assuming χ = 1 could be explained by a dependence of shape factor on particle size, such that χ approaches 1.08 for dry particles less than 50 nm in diameter and decreases toward 1 for particles with larger diameters.[18] This type of deviation is also observed for the sea salts.

3.2. Particle Morphology. A difference in NaCl and sea salt particle morphology, shown in this study to be independent of particle production and drying methods, is one possible explanation for the lower observed CCN activity and the lower hygroscopic growth factor of sea salt compared to that of NaCl. The possibility of morphological differences was investigated using analyses of AR from electron microscopy. Figure S2 shows scanning electron micrographs of atomized NaCl particles and TMSS particles generated from bubble bursting. In general, the morphologies of NaCl and sea salt samples in this study agree with TEM observations by Peart and Evans, who collected dried sea salt particles from film drops produced from bubble bursting.[50]

Table S1 lists the AR calculated for each of the particle samples. The mean AR of PSL spheres verifies that they are the most spherical of the samples analyzed. Fuchs[51] provides an approach to convert AR to χ, but the particles must be assumed to be elliptical. Kumar et al.[52] found that this approach, used with mineral aerosol, resulted in values much lower than those determined from direct measurements. In this study, AR is not converted to corresponding χ values; they are provided solely for intercomparison. Data in Table S1 show that there is no distinct difference between AR values of NaCl and TMSS. However, AR is only one parameter of many that can be used to describe morphology from images, and the possibility still exists that sea salt particles are not identical to NaCl particles in shape. For example, Peart and Evans[50] note that there is some elongation of sea salt particles from film drops and suggest that this is due to the presence of Na_2SO_4, a constituent of sea salt whose crystals tend to have a rod-like shape. Further studies should be conducted to investigate the possibility that interactions between the multiple inorganic constituents of sea salt lead to irregular particle morphologies, such as a higher than expected porosity or concave surfaces with high curvatures that may result in condensation at higher observed supersaturations.

3.3. Bubble-Bursting in Mixed Salt-Organic Solutions. In the oceans, the sea surface microlayer is enriched in organic compounds relative to the subsurface bulk seawater,[53] for which one of many explanations may be input from bubble scavenging.[54] An initial assumption may be that the further a bubble travels through seawater, the larger the potential for the bubble to collect organic molecules suspended in the water. A thorough discussion of the challenges of replicating oceanic bubble residence times in the laboratory is found in Fuentes et al.,[6] who calculate that the time required for adsorption equilibrium to be reached is less than 0.05 ms, much shorter than typical bubble residence times in laboratory-scale sea spray tanks. This implies that properties of particles produced in sea spray tanks would not differ for varying bubble residence times longer than 0.05 ms.

We probe the effect of bubble residence time in our study by measuring CCN activity and size distribution for different bubble rise distances (RD). Bubbles were produced using the diffuser, whose height was adjusted in the water column of the tank between 2.5 and 26.5 cm below the water surface. The residence times in the bulk artificial seawater solution of bubbles in the size range measured by the bubble spectrometer (Figure 1) were calculated using the parametrization of Clift et al.[55] (Figure S3). The artificial seawater in the tank was a two-component mixture of varying mass ratios, where one component was salt and the second was an organic compound. Details of each experiment are listed in Table 1.

Table 1. Experimental Conditions of Bubble-Bursting Experiments

experiment number	salt	organic	diffuser depth (cm below water surface)
1	0.27 g NaCl	1 g NaLa	2.5
2	0.27 g NaCl	1 g NaLa	26.5
3	60 g NaCl	1 g NaLa	2.5
4	60 g NaCl	1 g NaLa	26.5
5	350 g TMSS	0.5 g NaLa	2.5
6	350 g TMSS	0.5 g NaLa	14.5
7	350 g TMSS	0.5 g NaLa	26.5
8	350 g TMSS	35 g Fr	2.5
9	350 g TMSS	35 g Fr	26.5
10	350 g TMSS	0.05 g SDS	2.5
11	350 g TMSS	0.05 g SDS	26.5
12	350 g TMSS	0.01 g PA	26.5
13	100 g NaCl	1 g NaLa	26.5
14	100 g NaCl	1 g NaLa	Jet
15	100 g NaCl	1 g Ma	Jet

Number size distributions from Exps. 5−11 are shown in Figure 3. The shapes of the size distributions are similar for all

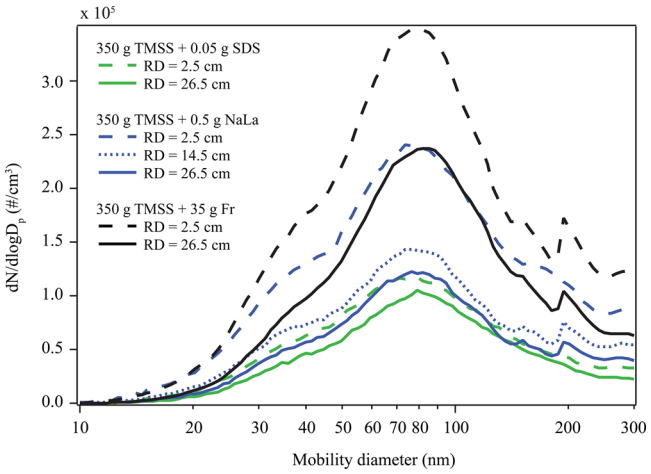

Figure 3. Number size distributions of particles produced from the diffuser at different depths (i.e., bubble RD) in the tank water column.

diffuser depths and organic compounds presented, with the exception of a small second mode near 200 nm. The presence of a smaller mode near 200 nm was also observed by Allan et al., who reported measurements in a marine environment of Puerto Rico.[56] Another general observation in Figure 3 is the reduction in particle number concentration in the presence of stronger surfactants. We ascribe this to the surface layer being significantly more stable, resulting in less bubble bursting in the case of SDS than in the case of fructose.

Figure 4a shows CCN activities from Exps. 1−4, in which NaCl and NaLa were added to the solutions. The results show that there is no significant difference in CCN activity between the two RDs studied. There is arguably a slight decrease in CCN activity at small particle sizes from Exp. 3 (shorter RD) to Exp. 4 (longer RD), but this should be further investigated using more direct methods for characterizing aerosol composition. The reduction in CCN activity from that of pure NaCl in Exps. 1 and 2 is not surprising, given the larger mass fraction of organic matter over NaCl in the artificial seawater.

Similar experiments were conducted using other organic molecules and a higher concentration of salt that is more typical of oceanic conditions. The results (Figure 4b) are again not significantly dependent on RD. Moreover, they are indistinguishable from the observed CCN activity of TMSS, even in Exps. 8 and 9, in which the mass contribution of fructose is 10% that of TMSS. This indicates that the contribution of salt in the particle phase determines the CCN activity, as expected given the nonlinear effect of particle salt composition on CCN activity.[16] Due to the minimal effect of organic molecules on CCN activity, these results cannot determine whether or not typical bubble residence times in sea spray tanks are sufficient for organic molecules to reach adsorption equilibrium on bubble surfaces. More direct measurements of aerosol composition in the future are recommended to further address these questions.

The production of particles from bubble bursting may also be affected by the possibility of a concentration gradient as a function of depth in the artificial seawater, especially in the case of surfactant molecules with limited water solubility. The addition of salt has the effect of lowering water solubility further and has in fact long been known to lower the critical micelle concentration of surfactants in aqueous solution,[57] which would result in a larger concentration of surfactant molecules at the air−water interface. If the organic matter in the water were concentrated near the surface, then bubble residence time in the subsurface seawater solution would presumably be insignificant in aerosol composition. This could further explain our observation that no large effect on CCN activity is observed with changes in bubble residence times. However, this explanation may be less relevant for experiments in which surfactants were not added.

The CCN activities of particles produced using the two methods of bubble generation are compared in Figure 4c (Exps. 13−15). The artificial seawater solution in these experiments contained 100 g of NaCl and 1 g of either NaLa or mannose. Number size distributions were measured (Figure 4c inset). The concentration of particles from jet-generated bubbles is considerably lower than that from diffuser-generated bubbles, and the distribution is broader and shifted toward slightly larger diameters. Submicrometer particles from jet impingement through a 4-mm nozzle on a seawater solution with NaLa are less CCN active than those from the diffuser, for all superaturations investigated (corresponding to activation diameters between 52 and 112 nm). For example, at 0.3% supersaturation, the activation diameter for a particle produced using the diffuser is 52 ± 2 nm, only minimally larger than the activation diameter of a NaCl particle (cf. Figure 2 for observed activation diameters of NaCl particles as well as calculated activation diameters for various χ), while the same for a particle produced using the jet is 93 ± 4 nm. On the other hand, submicrometer particles from jet impingement on a solution containing NaCl and mannose do not exhibit a similar reduction in CCN activity relative to pure salt particles.

Visual inspection of the sea spray tank during experiments with NaLa revealed that there was a foam layer floating on the surface of the artificial seawater and that the foam layer was much thicker during jet impingement. The liquid flow rate of the plunging jet was approximately 4 L min^{-1}, and the velocity of the liquid exiting the nozzle was approximately 5 m s^{-1}. Higher flow rates were avoided, as they resulted in the foam layer filling the headspace. Jet impingement on the solution containing NaCl and mannose did not result in a foam layer.

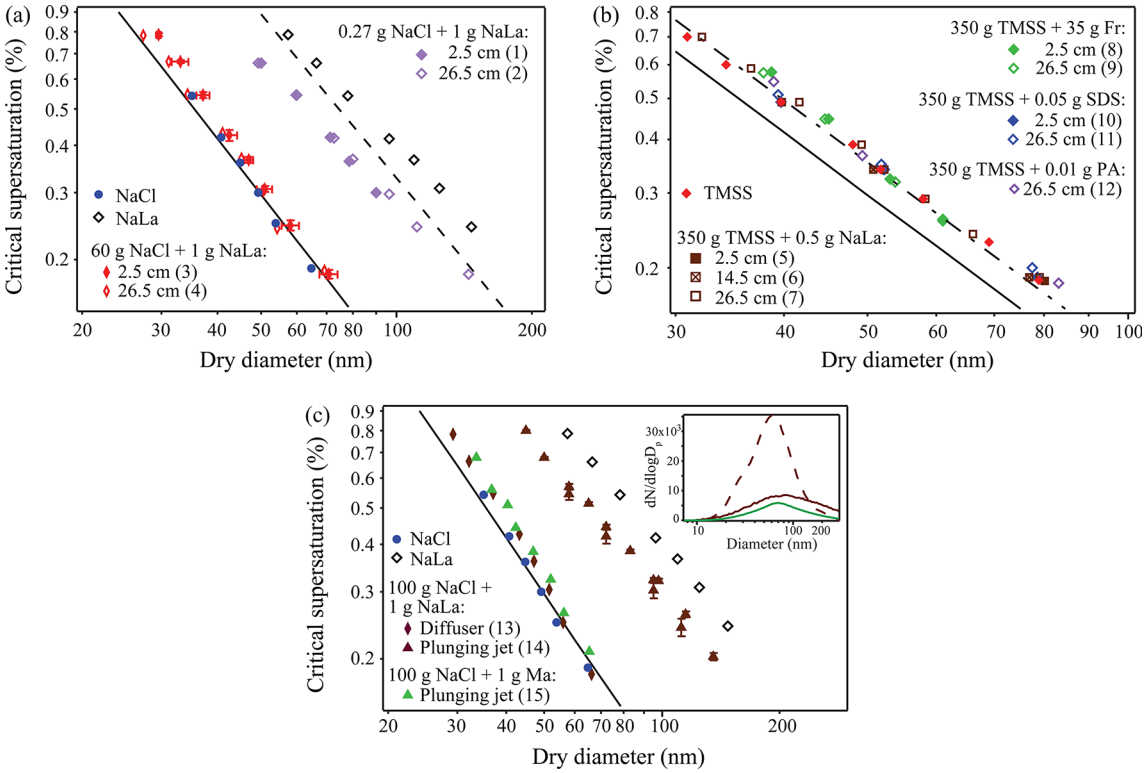

Figure 4. Observed CCN activities of particles produced in the sea spray tank from artificial seawater containing salt and one organic compound. Typical uncertainties are shown in panel a and were calculated as described in the caption for Figure 2. Experiment numbers corresponding to Table 1 are shown in parentheses in the legends. The solid line shows predicted S_c for NaCl with no correction for shape factor. (a) Measurements from seawater containing NaCl and NaLa. Depths of bubble generation from the diffuser are indicated in the legend. Measurements from diffuser-generated bubbles in solutions containing only NaCl and only NaLa are included for reference. The dashed line shows the parametrization of Prisle et al. based on measured CCN activities of NaLa particles atomized from an aqueous solution.[62] (b) Additional CCN measurements for varying depths of the diffuser below water surface. The artificial seawater in these experiments has a salinity (TMSS) of 35‰. The dashed line shows S_c calculated for NaCl particles with a shape factor of 1.24, which most closely agreed with observed measurements of sea salt particles (see Figure 2). (c) Comparison of the two bubble generation methods using CCN measurements. Data from Exps. 13−15 are shown, along with observed CCN data of pure NaCl and pure NaLa particles from diffuser-generated bubbles. Inset: Number size distributions from the same experiments, where the dashed line represents data obtained from the diffuser, and the solid line represents data obtained using the jet.

Given the absence of a significant reduction in observed CCN activity from jet impingement in Exp. 15, it may be concluded that a foam layer continuously ruptured and recreated by a plunging jet, which is the primary difference separating the two bubble generation methods, results in an aerosol population with a very different composition.

The observed difference in CCN activation between the two bubble generation methods is in agreement with observations by Fuentes et al.,[6] who reported an increase of 17% in S_c relative to that of NaCl when a plunging jet was used to generate particles from a tank with a solution containing T. rotula exudate (512 μM dissolved organic carbon (DOC) concentration). By comparison, S_c increased by only 11% when a porous bubbler was used. We speculate that the difference, though small as a consequence of low DOC, could be explained by dissimilar foam formation under the two bubbling methods.

The organic fraction of particles formed from jet-generated bubbles can be roughly estimated by comparing the observed CCN data with measurements by Prisle et al.[58] of mixed NaCl-NaLa particles whose fractional composition was systematically varied. The comparison suggests that the particles are composed of approximately 80% (by mass) NaLa. This is an approximation and is most likely dependent on particle size. Nevertheless, it strongly indicates organic enrichment, since the solute in the bulk seawater solution is only 1% (by mass) NaLa.

The hygroscopicity parameter κ was also calculated for these experiments. In Exp. 14, κ ranges from 0.16 to 0.23, values that are considerably lower than those typical of NaCl. On the other hand, κ in Exp. 13 ranges from 0.89 to 1.41; these higher values are similar to κ calculated for NaCl particles having various shape factors.

The above results lead to the conclusion that, while there is little to no detectable effect from variations in residence times of bubbles from diffuser aeration, the CCN activity of submicrometer particles produced by jet impingement on artificial seawater containing an organic surfactant is substantially lower than that of diffuser-generated submicrometer particles from the same seawater solution. This indicates that bubble production methods used in sea spray tanks for aerosol studies are not equal, particularly when the seawater in the tank includes organic surfactants. Findings from this study as well as others using bubble spectra[6,8,25] suggest that the more appropriate method would be the plunging jet. Furthermore, our results suggest that formation of a stable foam layer can significantly change the chemical composition and CCN properties of sea spray particles compared to the properties of particles generated from the same water in the absence of foam. Given the ubiquitous nature of surfactants in the marine environment and the large fraction of ocean surface covered by

foam, or whitecap, conditions,[59−61] these considerations potentially affect a large number of future studies.

■ ASSOCIATED CONTENT

Supporting Information

Table S1 and Figures S1−S3. This material is available free of charge via the Internet at http://pubs.acs.org.

■ AUTHOR INFORMATION

Corresponding Author

*Phone: +45 35320329. E-mail: mbilde@chem.ku.dk.

Present Address

[▽]FORCE Technology, Park Allé 345, DK-2605 Brøndby, Denmark.

Notes

The authors declare no competing financial interest.

■ ACKNOWLEDGMENTS

This work is supported by the Carlsberg Foundation (Grant 2009_01_0515), the Swedish Research Council, and the CRAICC (Cryosphere-Atmosphere Interactions in a Changing Arctic Climate) project. We thank Erik Johnson of the Niels Bohr Institute for providing the TEM.

■ REFERENCES

(1) Textor, C.; Schulz, M.; Guibert, S.; Kinne, S.; Balkanski, Y.; Bauer, S.; Berntsen, T.; Berglen, T.; Boucher, O.; Chin, M.; Dentener, F.; Diehl, T.; Easter, R.; Feichter, H.; Fillmore, D.; Ghan, S.; Ginoux, P.; Gong, S.; Kristjansson, J. E.; Krol, M.; Lauer, A.; Lamarque, J. F.; Liu, X.; Montanaro, V.; Myhre, G.; Penner, J.; Pitari, G.; Reddy, S.; Seland, O.; Stier, P.; Takemura, T.; Tie, X. Analysis and quantification of the diversities of aerosol life cycles within AeroCom. *Atmos. Chem. Phys.* **2006**, *6*, 1777−1813.

(2) Fitzgerald, J. W. Marine aerosols: A review. *Atmos. Environ., Part A* **1991**, *25*, 533−545.

(3) Cavalli, F.; Facchini, M. C.; Decesari, S.; Mircea, M.; Emblico, L.; Fuzzi, S.; Ceburnis, D.; Yoon, Y. J.; O'Dowd, C. D.; Putaud, J. P; Dell'Acqua, A. Advances in characterization of size-resolved organic matter in marine aerosol over the North Atlantic. *J. Geophys. Res., [Atmos.]* **2004**, *109* (D24), DOI 10.1029/2004jd005137.

(4) Keene, W. C.; Maring, H.; Maben, J. R.; Kieber, D. J.; Pszenny, A. A. P.; Dahl, E. E.; Izaguirre, M. A.; Davis, A. J.; Long, M. S.; Zhou, X. L.; Smoydzin, L.; Sander, R. Chemical and physical characteristics of nascent aerosols produced by bursting bubbles at a model air-sea interface. *J. Geophys. Res., [Atmos.]* **2007**, *112* (D21), DOI 10.1029/2007jd008464.

(5) Facchini, M. C.; Rinaldi, M.; Decesari, S.; Carbone, C.; Finessi, E.; Mircea, M.; Fuzzi, S.; Ceburnis, D.; Flanagan, R.; Nilsson, E. D.; de Leeuw, G.; Martino, M.; Woeltjen, J.; O'Dowd, C. D. Primary submicron marine aerosol dominated by insoluble organic colloids and aggregates. *Geophys. Res. Lett.* **2008**, *35* (17), DOI 10.1029/2008gl034210.

(6) Fuentes, E.; Coe, H.; Green, D.; de Leeuw, G.; McFiggans, G. Laboratory-generated primary marine aerosol via bubble-bursting and atomization. *Atmos. Meas. Tech.* **2010**, *3* (1), 141−162.

(7) Mårtensson, E. M.; Nilsson, E. D.; de Leeuw, G.; Cohen, L. H.; Hansson, H. C. Laboratory simulations and parameterization of the primary marine aerosol production. *J. Geophys. Res., [Atmos.]* **2003**, *108* (D9), DOI 10.1029/2002jd002263.

(8) Sellegri, K.; O'Dowd, C. D.; Yoon, Y. J.; Jennings, S. G.; de Leeuw, G. Surfactants and submicron sea spray generation. *J. Geophys. Res., [Atmos.]* **2006**, *111* (D22), DOI 10.1029/2005jd006658.

(9) Tyree, C. A.; Hellion, V. M.; Alexandrova, O. A.; Allen, J. O. Foam droplets generated from natural and artificial seawaters. *J. Geophys. Res., [Atmos.]* **2007**, *112* (D12), DOI 10.1029/2006jd007729.

(10) O'Dowd, C. D.; Smith, M. H.; Consterdine, I. E.; Lowe, J. A. Marine aerosol, sea-salt, and the marine sulphur cycle: A short review. *Atmos. Environ.* **1997**, *31* (1), 73−80.

(11) Latham, J.; Smith, M. H. Effect on global warming of wind-dependent aerosol generation at the ocean surface. *Nature* **1990**, *347* (6291), 372−373, DOI: 10.1038/347372a0.

(12) Novakov, T.; Penner, J. E. Large contribution of organic aerosols to cloud-condensation-nuclei concentrations. *Nature* **1993**, *365* (6449), 823−826, DOI: 10.1038/365823a0.

(13) IPCC, *Climate Change 2007 - The Physical Science Basis: Contribution of Working Group I to the Fourth Assessment Report of the IPCC*; Cambridge University Press: UK, 2007.

(14) Fuentes, E.; Coe, H.; Green, D.; McFiggans, G. On the impacts of phytoplankton-derived organic matter on the properties of the primary marine aerosol - Part 2: Composition, hygroscopicity and cloud condensation activity. *Atmos. Chem. Phys.* **2011**, *11* (6), 2585−2602, DOI: 10.5194/Acp-11-2585-2011.

(15) Moore, M. J. K.; Furutani, H.; Roberts, G. C.; Moffet, R. C.; Gilles, M. K.; Palenik, B.; Prather, K. A. Effect of organic compounds on cloud condensation nuclei (CCN) activity of sea spray aerosol produced by bubble bursting. *Atmos. Environ.* **2011**, *45* (39), 7462−7469, DOI: 10.1016/J.Atmosenv.2011.04.034.

(16) Bilde, M.; Svenningsson, B. CCN activation of slightly soluble organics: the importance of small amounts of inorganic salt and particle phase. *Tellus Ser., B* **2004**, *56* (2), 128−134, DOI: 10.1111/j.1600-0889.2004.00090.x.

(17) Biskos, G.; Russell, L. M.; Buseck, P. R.; Martin, S. T. Nanosize effect on the hygroscopic growth factor of aerosol particles. *Geophys. Res. Lett.* **2006**, *33* (7), DOI 10.1029/2005gl025199.

(18) Wang, Z.; King, S. M.; Freney, E.; Rosenoern, T.; Smith, M. L.; Chen, Q.; Kuwata, M.; Lewis, E. R.; Poschl, U.; Wang, W.; Buseck, P. R.; Martin, S. T. The Dynamic Shape Factor of Sodium Chloride Nanoparticles as Regulated by Drying Rate. *Aerosol Sci. Technol.* **2010**, *44* (11), 939−953, DOI: 10.1080/02786826.2010.503204.

(19) de Leeuw, G.; Andreas, E. L.; Anguelova, M. D.; Fairall, C. W.; Lewis, E. R.; O'Dowd, C.; Schulz, M.; Schwartz, S. E. Production Flux of Sea Spray Aerosol. *Rev. Geophys.* **2011**, 49 DOI: 10.1029/2010rg000349.

(20) Bin, A. K. Gas entrainment by plunging liquid jets. *Chem. Eng. Sci.* **1993**, *48* (21), 3585−3630, DOI: 10.1016/0009-2509(93)81019-r.

(21) Chanson, H.; Aoki, S.; Hoque, A. Physical modelling and similitude of air bubble entrainment at vertical circular plunging jets. *Chem. Eng. Sci.* **2004**, *59* (4), 747−758, DOI: 10.1016/j.ces.2003.11.016.

(22) Chanson, H.; Aoki, S.; Hoque, A. Bubble entrainment and dispersion in plunging jet flows: Freshwater vs. seawater. *J. Coastal Res.* **2006**, *22* (3), 664−677, DOI: 10.1212/03-0112.1.

(23) Evans, G. M.; Jameson, G. J.; Rielly, C. D. Free jet expansion and gas entrainment characteristics of a plunging liquid jet. *Exp. Therm. Fluid Sci.* **1996**, *12* (2), 142−149, DOI: 10.1016/0894-1777(95)00095-x.

(24) Leifer, I.; De Leeuw, G.; Cohen, L. H. Optical measurement of bubbles: System design and application. *J. Atmos. Ocean Tech.* **2003**, *20* (9), 1317−1332.

(25) Hutin, K. A. H.; Nilsson, E. D.; Krejci, R.; Martensson, E. M.; Ehn, M.; Hagstrom, A.; de Leeuw, G. In situ laboratory sea spray production during the Marine Aerosol Production 2006 cruise on the northeastern Atlantic Ocean. *J. Geophys. Res., [Atmos.]* **2010**, *115*, DOI 10.1029/2009jd012522.

(26) Deane, G. B.; Stokes, M. D. Scale dependence of bubble creation mechanisms in breaking waves. *Nature* **2002**, *418* (6900), 839−844, DOI: 10.1038/nature00967.

(27) Bowyer, P. A. Video measurements of near-surface bubble spectra. *J. Geophys. Res., [Oceans]* **2001**, *106* (C7), 14179−14190.

(28) Deane, G. B.; Stokes, M. D. Air entrainment processes and bubble size distributions in the surf zone. *J. Phys. Oceanogr.* **1999**, *29* (7), 1393−1403, DOI: 10.1175/1520-0485(1999)029<1393:aepabs>2.0.co;2.

(29) Kester, D. R.; Duedall, I. W.; Connors, D. N.; Pytkowic, R. M. Preparation of Artificial Seawater. *Limnol. Oceanogr.* **1967**, *12* (1), 176−179.
(30) Mochida, M.; Kitamori, Y.; Kawamura, K.; Nojiri, Y.; Suzuki, K. Fatty acids in the marine atmosphere: Factors governing their concentrations and evaluation of organic films on sea-salt particles. *J. Geophys. Res., [Atmos.]* **2002**, *107* (D17), DOI 10.1029/2001jd001278.
(31) Russell, L. M.; Hawkins, L. N.; Frossard, A. A.; Quinn, P. K.; Bates, T. S. Carbohydrate-like composition of submicron atmospheric particles and their production from ocean bubble bursting. *Proc. Natl. Acad. Sci. U.S.A.* **2010**, *107* (15), 6652−6657, DOI: 10.1073/pnas.0908905107.
(32) Coz, E.; Gomez-Moreno, F. J.; Casuccio, G. S.; Artinano, B. Variations on morphology and elemental composition of mineral dust particles from local, regional, and long-range transport meteorological scenarios. *J. Geophys. Res., [Atmos.]* **2010**, *115*, DOI 10.1029/2009jd012796.
(33) Coz, E.; Gomez-Moreno, F. J.; Pujadas, M.; Casuccio, G. S.; Lersch, T. L.; Artinano, B. Individual particle characteristics of North African dust under different long-range transport scenarios. *Atmos. Environ.* **2009**, *43* (11), 1850−1863, DOI: 10.1016/J.Atmosenv.2008.12.045.
(34) Kandler, K.; Benker, N.; Bundke, U.; Cuevas, E.; Ebert, M.; Knippertz, P.; Rodriguez, S.; Schutz, L.; Weinbruch, S. Chemical composition and complex refractive index of Saharan Mineral Dust at Izana, Tenerife (Spain) derived by electron microscopy. *Atmos. Environ.* **2007**, *41* (37), 8058−8074, DOI: 10.1016/J.Atmosenv.2007.06.047.
(35) Adachi, K.; Buseck, P. R. Internally mixed soot, sulfates, and organic matter in aerosol particles from Mexico City. *Atmos. Chem. Phys.* **2008**, *8* (21), 6469−6481.
(36) Chakrabarty, R. K.; Moosmuller, H.; Arnott, W. P.; Garro, M. A.; Walker, J. Structural and fractal properties of particles emitted from spark ignition engines. *Environ. Sci. Technol.* **2006**, *40* (21), 6647−6654, DOI: 10.1021/Es060537y.
(37) Chakrabarty, R. K.; Moosmuller, H.; Garro, M. A.; Arnott, W. P.; Walker, J.; Susott, R. A.; Babbitt, R. E.; Wold, C. E.; Lincoln, E. N.; Hao, W. M. Emissions from the laboratory combustion of wildland fuels: Particle morphology and size. *J. Geophys. Res., [Atmos.]* **2006**, *111* (D7), DOI 10.1029/2005jd006659.
(38) Otto, S.; Trautmann, T.; Wendisch, M. On realistic size equivalence and shape of spheroidal Saharan mineral dust particles applied in solar and thermal radiative transfer calculations. *Atmos. Chem. Phys.* **2011**, *11* (9), 4469−4490, DOI: 10.5194/Acp-11-4469-2011.
(39) Petters, M. D.; Prenni, A. J.; Kreidenweis, S. M.; DeMott, P. J. On measuring the critical diameter of cloud condensation nuclei using mobility selected aerosol. *Aerosol Sci. Technol.* **2007**, *41* (10), 907−913, DOI: 10.1080/02786820701557214.
(40) Rose, D.; Gunthe, S. S.; Mikhailov, E.; Frank, G. P.; Dusek, U.; Andreae, M. O.; Poschl, U. Calibration and measurement uncertainties of a continuous-flow cloud condensation nuclei counter (DMT-CCNC): CCN activation of ammonium sulfate and sodium chloride aerosol particles in theory and experiment. *Atmos. Chem. Phys.* **2008**, *8* (5), 1153−1179.
(41) The Extended Aerosol Inorganics Model Project. http://www.aim.env.uea.ac.uk/aim/aim.html (accessed multiple times from 2010 to 2011).
(42) Clegg, S. L.; Brimblecombe, P.; Wexler, A. S. Thermodynamic model of the system H+-NH4+-Na+-SO42−NB3−Cl−H2O at 298.15 K. *J. Phys. Chem. A* **1998**, *102* (12), 2155−2171.
(43) Modini, R. L.; Harris, B.; Ristovski, Z. D. The organic fraction of bubble-generated, accumulation mode Sea Spray Aerosol (SSA). *Atmos. Chem. Phys.* **2010**, *10* (6), 2867−2877.
(44) Ming, Y.; Russell, L. M. Predicted hygroscopic growth of sea salt aerosol. *J. Geophys. Res., [Atmos.]* **2001**, *106* (D22), 28259−28274, DOI: 10.1029/2001jd000454.
(45) Harvie, C. E.; Moller, N.; Weare, J. H. The Prediction of Mineral Solubilities in Natural-Waters - the Na-K-Mg-Ca-H-Cl-So4-Oh-Hco3-Co3-Co2-H2o System to High Ionic Strengths at 25-Degrees-C. *Geochim. Cosmochim. Acta* **1984**, *48* (4), 723−751.
(46) Davis, C. N. Particle-fluid interaction. *J. Aerosol Sci.* **1979**, *10*, 477−513.
(47) Baron, P. A.; Willeke, K. *Aerosol Measurement: Principles, Techniques, and Applications*, 2nd ed.; John Wiley & Sons: New York, 2001.
(48) Charlesworth, D. H.; Marshall, W. R. Evaporation from Drops Containing Dissolved Solids. *AIChE J.* **1960**, *6* (1), 9−23.
(49) Lewis, E. R.; Schwartz, S. E. *Sea salt aerosol production: mechanisms, methods, measurements and models: a critical review*; American Geophysical Union: Washington, DC, 2004; p xii, 413 p.
(50) Peart, A.; Evans, J. R. G. Study of sea salt particles launched by bubble burst. *Bubble Sci., Eng., Technol.* **2011**, DOI: 10.1179/1758897911Y.0000000004.
(51) Fuchs, N. A. *The Mechanics of Aerosols*; Pergamon: New York, 1964.
(52) Kumar, P.; Sokolik, I. N.; Nenes, A. Measurements of cloud condensation nuclei activity and droplet activation kinetics of fresh unprocessed regional dust samples and minerals. *Atmos. Chem. Phys.* **2011**, *11* (7), 3527−3541, DOI: 10.5194/Acp-11-3527-2011.
(53) Hunter, K. A.; Liss, P. S. Input of organic material to oceans - air-sea interactions and organic chemical composition of sea-surface. *Mar. Chem.* **1977**, *5* (4−6), 361−379, DOI: 10.1016/0304-4203(77)90029-9.
(54) Liss, P. S.; Duce, R. A. *The Sea Surface and Global Change*; Cambridge University Press: Cambridge, 1997.
(55) Clift, R.; Grace, J. R.; Weber, M. E. *Bubbles, Drops, and Particles*; Academic Press: New York, 1978; p 380.
(56) Allan, J. D.; Baumgardner, D.; Raga, G. B.; Mayol-Bracero, O. L.; Morales-Garcia, F.; Garcia-Garcia, F.; Montero-Martinez, G.; Borrmann, S.; Schneider, J.; Mertes, S.; Walter, S.; Gysel, M.; Dusek, U.; Frank, G. P.; Kramer, M. Clouds and aerosols in Puerto Rico - a new evaluation. *Atmos. Chem. Phys.* **2008**, *8* (5), 1293−1309.
(57) Corrin, M. L.; Harkins, W. D. The Effect of Salts on the Critical Concentration for the Formation of Micelles in Colloidal Electrolytes. *J. Am. Chem. Soc.* **1947**, *69* (3), 683−688.
(58) Prisle, N. L.; Raatikainen, T.; Laaksonen, A.; Bilde, M. Surfactants in cloud droplet activation: mixed organic-inorganic particles. *Atmos. Chem. Phys.* **2010**, *10* (12), 5663−5683, DOI: 10.5194/Acp-10-5663-2010.
(59) Blanchard, D. C. Whitecap at sea. *J. Atmos. Sci.* **1971**, *28* (4), 645 DOI: 10.1175/1520-0469(1971)028<0645:was>2.0.co;2.
(60) Monahan, E. C.; Muircheartaigh, I. O. Optimal power-law description of oceanic whitecap coverage dependence on wind-speed. *J. Phys. Oceanogr.* **1980**, *10* (12), 2094−2099, DOI: 10.1175/1520-0485(1980)010<2094:opldoo>2.0.co;2.
(61) Wu, J. Oceanic whitecaps and sea state. *J. Phys. Oceanogr.* **1979**, *9* (5), 1064−1068, DOI: 10.1175/1520-0485(1979)009<1064:owass>2.0.co;2.
(62) Prisle, N. L.; Raatikainen, T.; Sorjamaa, R.; Svenningsson, B.; Laaksonen, A.; Bilde, M. Surfactant partitioning in cloud droplet activation: a study of C8, C10, C12 and C14 normal fatty acid sodium salts. *Tellus Ser., B* **2008**, *60* (3), 416−431, DOI: 10.1111/J.1600-0889.2008.00352.X.